THz emission from organic cocrystalline salt: 2, 6-diaminopyridinium-4-nitrophenolate-4-nitrophenol

Chien-Ming Tu,[1] Li-Hsien Chou,[1] Yi-Cheng Chen,[1] Ping Huang,[1] M. Rajaboopathi,[3,4] Chih-Wei Luo,[1,2,*] Kaung-Hsiung Wu,[1] V. Krishnakumar,[3] and Takayoshi Kobayashi[1,5,6]

[1]*Department of Electrophysics, National Chiao Tung University, Hsinchu 30010, Taiwan*
[2]*Taiwan Consortium of Emergent Crystalline Materials, Ministry of Science and Technology, Taipei 10601, Taiwan*
[3]*Department of Physics, Periyar University, Salem-636 011, Tamilnadu, India*
[4]*State Key Laboratory of Crystal Materials, Shandong University, Jinan 250100, China*
[5]*Advanced Ultrafast Laser Research Center, and Department of Engineering Science, Faculty of Informatics and Engineering, University of Electro-Communications, 1-5-1 Chofugaoka, Chofu, Tokyo 182-8585, Japan*
[6]*Institute of Laser Engineering, Osaka University, Osaka 565-0971, Japan*
[*]*cwluo@mail.nctu.edu.tw*

Abstract: We report few-cycle THz pulses emission from a novel organic crystal 2,6-diaminopyridinium-4-nitrophenolate-4-nitrophenol (DAP^+NP^-NP). The observed amplitude of the THz electric field from a DAP^+NP^-NP crystal is comparable with that from a ZnTe single crystal under the same optical pumping conditions. Both the waveform and spectra of the THz radiation from DAP^+NP^-NP are similar to those from ZnTe. We conclude that a high quality DAP^+NP^-NP crystal would be a high potential candidate in THz generation and applications.

OCIS codes: (190.7110) Ultrafast nonlinear optics; (160.4890) Organic materials.

References and links

1. B. Ferguson and X.-C. Zhang, “Materials for terahertz science and technology,” Nat. Mater. **1**(1), 26–33 (2002).
2. C. M. Tu, S. A. Ku, W. C. Chu, C. W. Luo, J. C. Chen, and C. C. Chi, “Pulsed terahertz radiation due to coherent phonon-polariton excitation in <110> ZnTe crystal,” J. Appl. Phys. **112**(9), 093110 (2012).
3. S. A. Ku, C. M. Tu, W.-C. Chu, C. W. Luo, K. H. Wu, A. Yabushita, C. C. Chi, and T. Kobayashi, “Saturation of the free carrier absorption in ZnTe crystals,” Opt. Express **21**(12), 13930–13937 (2013).
4. W.-C. Chu, S. A. Ku, H. J. Wang, C. W. Luo, Y. M. Andreev, G. Lanskii, and T. Kobayashi, “Widely linear and non-phase-matched optical-to-terahertz conversion on GaSe:Te crystals,” Opt. Lett. **37**(5), 945–947 (2012).
5. S. A. Ku, W.-C. Chu, C. W. Luo, Y. M. Andreev, G. Lanskii, A. Shaidukoi, T. Izaak, V. Svetlichnyi, K. H. Wu, and T. Kobayashi, “Optimal Te-doping in GaSe for non-linear applications,” Opt. Express **20**(5), 5029–5037 (2012).
6. J. Hebling, K. L. Yeh, M. C. Hoffmann, B. Bartal, and K. A. Nelson, “Generation of high-power terahertz pulses by tilted-pulse-front excitation and their application possibilities,” J. Opt. Soc. Am. B **25**(7), B6–B19 (2008).
7. A. G. Stepanov, L. Bonacina, S. V. Chekalin, and J.-P. Wolf, “Generation of 30 microJ single-cycle terahertz pulses at 100 Hz repetition rate by optical rectification,” Opt. Lett. **33**(21), 2497–2499 (2008).
8. C. P. Hauri, C. Ruchert, C. Vicario, and F. Ardana, “Strong-field single-cycle THz pulses generated in an organic crystal,” Appl. Phys. Lett. **99**(16), 161116 (2011).
9. C. Vicario, B. Monoszlai, and C. P. Hauri, “GV/m single-cycle terahertz fields from a laser-driven large-size partitioned organic crystal,” Phys. Rev. Lett. **112**(21), 213901 (2014).
10. C. Ruchert, C. Vicario, and C. P. Hauri, “Scaling submillimeter single-cycle transients toward megavolts per centimeter field strength via optical rectification in the organic crystal OH1,” Opt. Lett. **37**(5), 899–901 (2012).
11. V. Krishnakumar, M. Rajaboopathi, and R. Nagalakshmi, “Studies on vibrational, dielectric, mechanical and thermal properties of organic nonlinear optical co-crystal: 2,6-diaminopyridinium–4-nitrophenolate–4-nitrophenol,” Physica B **407**(7), 1119–1123 (2012).
12. M. J. Prakash and T. P. Radhakrishnan, “SHG active salts of 4-nitrophenolate with h-bonded helical formations: structure-directing role of ortho-aminopyridines,” Cryst. Growth Des. **5**(2), 721–725 (2005).
13. T. Chen, Z. Sun, L. Li, S. Wang, Y. Wang, J. Luo, and M. Hong, “Growth and characterization of a nonlinear optical crysta - 2,6-diaminopyridinium 4-nitrophenolate 4-nitrophenol (DAPNP),” J. Cryst. Growth **338**(1), 157–161 (2012).
14. http://www.crystallography.net/cod/4505002.html

#254193 Received 18 Nov 2015; revised 10 Feb 2016; accepted 17 Feb 2016; published 29 Feb 2016

15. J. Zyss and D. S. Chemla, "Quadratic nonlinear optics and optimization of the second-order nonlinear optical response of molecular crystals," in *Nonlinear Optical Properties of Organic Molecules and Crystals*, D. S. Chemla, ed. (Academic Press, 1987).
16. J. Ahn, A. Efimov, R. Averitt, and A. Taylor, "Terahertz waveform synthesis via optical rectification of shaped ultrafast laser pulses," Opt. Express **11**(20), 2486–2496 (2003).

1. Introduction

Few-cycle terahertz (THz) electromagnetic pulses have attracted much attention because they have high potential in fundamental studies and practical applications [1]. Inorganic crystals, such as ZnTe, GaSe:Te, used as THz emitters equipped with ultrafast lasers have become popular and high signal-to-noise ratio tabletop THz sources around the world [2–5]. Recently, intense THz pulses have been demonstrated in $LiNbO_3$ by using tilted pulse front excitation, which has extended the applications of THz radiation into the nonlinear region [6,7]. On the other hand, due to large second-order nonlinear susceptibilities and low dielectric constants for phase-matching, organic nonlinear optical crystals have received much more attention for THz generation. Some organic crystals such as DAST, DSTMS and OH1 have been applied to high-field THz generation [8–10]. However, due to low frequency phonon/resonance absorption in the THz frequency range, the waveforms and spectra of THz emission from these novel organic crystals are distorted and hence not preferable in some applications. Therefore, ZnTe or $LiNbO_3$ incorporated with Ti:sapphire lasers are still the most popular THz emitters currently.

In this study, we demonstrate THz emission from a novel organic crystal 2,6-diaminopyridinium-4-nitrophenolate-4-nitrophenol (DAP^+NP^-NP) [11–13]. The field strength of the THz emission from a DAP^+NP^-NP crystal is comparable with that from a typical THz emitter-ZnTe crystal. Few-cycle THz pulses were observed from a DAP^+NP^-NP crystal, and both the waveform and spectra from DAP^+NP^-NP are similar to those from ZnTe.

2. Sample preparation and THz emission experiments

The DAP^+NP^-NP crystals used in this study were synthesized by slow-evaporation-solution method with ethanol as a solvent [11]. A photo of the used crystal is shown in the inset of Fig. 1(a) and the thickness of the sample is ~0.41 mm. We used the XRD θ-2θ scan method to determine the orientation of the used crystal. As shown in Fig. 1(a), three diffraction peaks appear at 16.28°, 33.30° and 50.66°. By comparing with structure in the crystallography database, we confirm that these peaks correspond to the diffracted peaks of (200), (400) and (600), respectively [14]. Therefore, the result of XRD θ-2θ scan suggests that the surface normal of the used crystal is approximately along the <100>-direction.

In the transmission-configuration THz generation experiments, a commercial Ti:sapphire oscillator (Femtosource scientific XL300, FEMTOLASERS Produktions GmbH) operating at a central wavelength of 800 nm was employed as a pumping source and it produced optical pulses of 100 fs at a repetition rate of 5.2 MHz. The pump beam was focused on the samples in a diameter of ~150 μm and pulse energy of 70.7 nJ to generate THz radiation. The transmitted THz radiation was collimated by two off-axis parabolic mirrors and focused on a 1-mm-thick <110> ZnTe slab for electro-optic sampling. All experiments were performed in a chamber filled with dry nitrogen gas at room temperature.

3. Results and discussion

Figure 1(b) shows the THz temporal waveforms generated from the DAP^+NP^-NP crystal in different polarization-configurations. In the $P_{Opt}//P_{THz}$ configuration, i.e., the polarizations of optical pulses and THz radiation were parallel to each other, a few-cycle THz pulse (black line) can be clearly observed and the maximum amplitude of electric field is denoted as $E_{O//T}^{DAP^+NP^-NP}$. As the polarization of optical pulses was perpendicular to that of THz radiation, in the $P_{Opt}\perp P_{THz}$ configuration, a THz pulse with the same temporal shape (red line vs. black line) and an amplitude of about twice larger, i.e., $E_{O\perp T}^{DAP^+NP^-NP} / E_{O//T}^{DAP^+NP^-NP} = 1.56 / 0.72 = 2.17$,

#254193 Received 18 Nov 2015; revised 10 Feb 2016; accepted 17 Feb 2016; published 29 Feb 2016

was obtained. In the experiments, we also used a 1-mm-thick <110> ZnTe slab to generate THz radiation, under the same conditions as in $P_{Opt}//P_{THz}$ configuration. As seen clearly in the figure, the amplitude of the electric field from the ZnTe slab is about six-times larger than that from the DAP$^+$NP$^-$NP crystal ($E_{O//T}^{ZnTe} / E_{O//T}^{DAP^+NP^-NP} = 4.50/0.72 = 6.25$) in the $P_{Opt}//P_{THz}$ configuration.

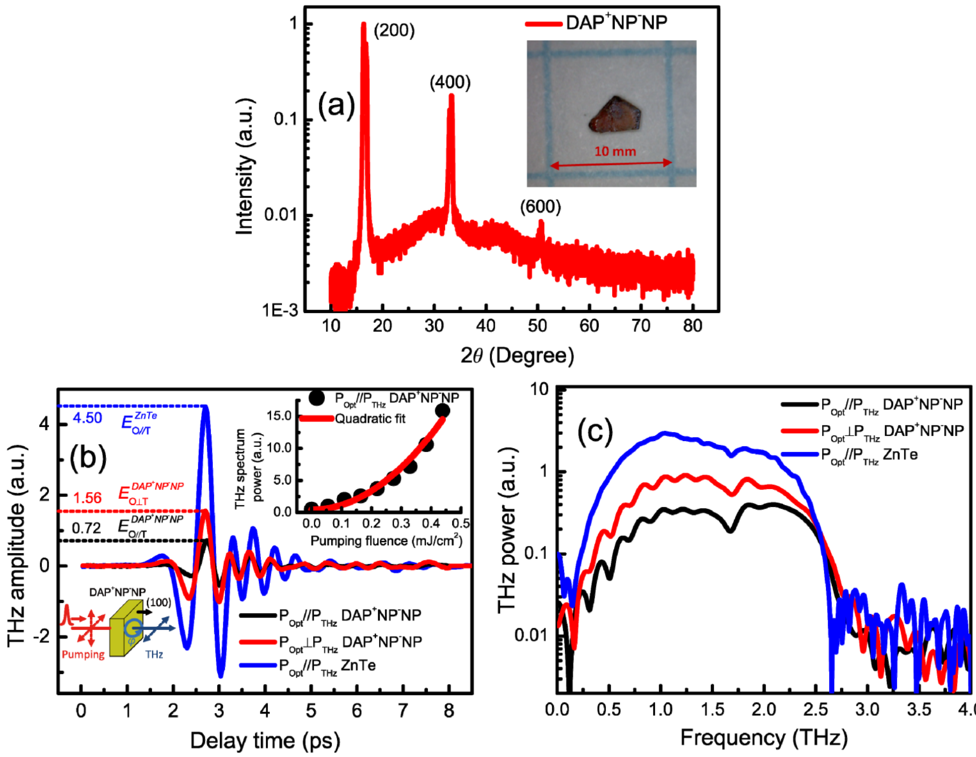

Fig. 1. (a) X-ray diffraction θ-2θ scan results of the employed DAP$^+$NP$^-$NP crystal. Comparing with crystallography Database, the diffraction peaks at 16.28°, 33.31° and 50.66° correspond to the diffracted peaks of (200), (400) and (600), respectively [14]. The surface normal of the employed DAP$^+$NP$^-$NP crystal is approximately (100). The inset shows the photo of the employed crystal. (b) THz waveforms from a DAP$^+$NP$^-$NP crystal in the configurations of $P_{Opt}//P_{THz}$ (black) and $P_{Opt}\perp P_{THz}$ (red). The THz waveform from 1-mm <110> ZnTe in the configuration of $P_{Opt}//P_{THz}$ (blue) is also shown as a reference. The inset shows the experimental configuration and the pumping fluence dependence of THz radiation from a DAP$^+$NP$^-$NP crystal (black point) and the quadratic fitting (red line) in $P_{Opt}//P_{THz}$ configuration. (c) The corresponding THz emission spectra.

The FFT spectra of the temporal waveforms are shown in Fig. 1(c). We find that the spectra from a DAP$^+$NP$^-$NP crystal (both $P_{Opt}//P_{THz}$ and $P_{Opt}\perp P_{THz}$) show comparable bandwidth to those from 1-mm-thick ZnTe. We also perform pumping fluence-dependent experiments to investigate the mechanism of THz generation from the DAP$^+$NP$^-$NP crystal. As shown in the inset of Fig. 1(b), the THz spectrum power in the $P_{Opt}//P_{THz}$ configuration shows quadric dependence on the pumping fluence, which indicates that the THz generation in the DAP$^+$NP$^-$NP crystal is due to the second-order nonlinear optical effect.

To gain more insight into the mechanism of THz generated from a DAP$^+$NP$^-$NP crystal, we rotated the DAP$^+$NP$^-$NP crystal to perform azimuthal angle scan (ϕ -scan) measurements in the both $P_{Opt}//P_{THz}$ and $P_{Opt}\perp P_{THz}$ configurations, as shown in Figs. 2(c) and 2(d), respectively. In the left part of Fig. 2(c), the THz power ϕ -scan result reveals six-fold symmetry in the $P_{Opt}//P_{THz}$ configuration. However, by THz waveform polarity analysis (the

#254193 Received 18 Nov 2015; revised 10 Feb 2016; accepted 17 Feb 2016; published 29 Feb 2016

polarity states are marked by "+/–"), although the polarity of the THz waveform reverses under 180°-rotation of the employed crystal, the polarity ϕ-scan does not follow six-fold symmetry; that is, the polarity of the THz waveform should reverse under 60°-rotation. On the other hand, in the left of Fig. 2(d), the THz power ϕ-scan result shows two-fold symmetry in the $P_{Opt}{\perp}P_{THz}$ configuration and the polarity also reverses under 180°-rotation.

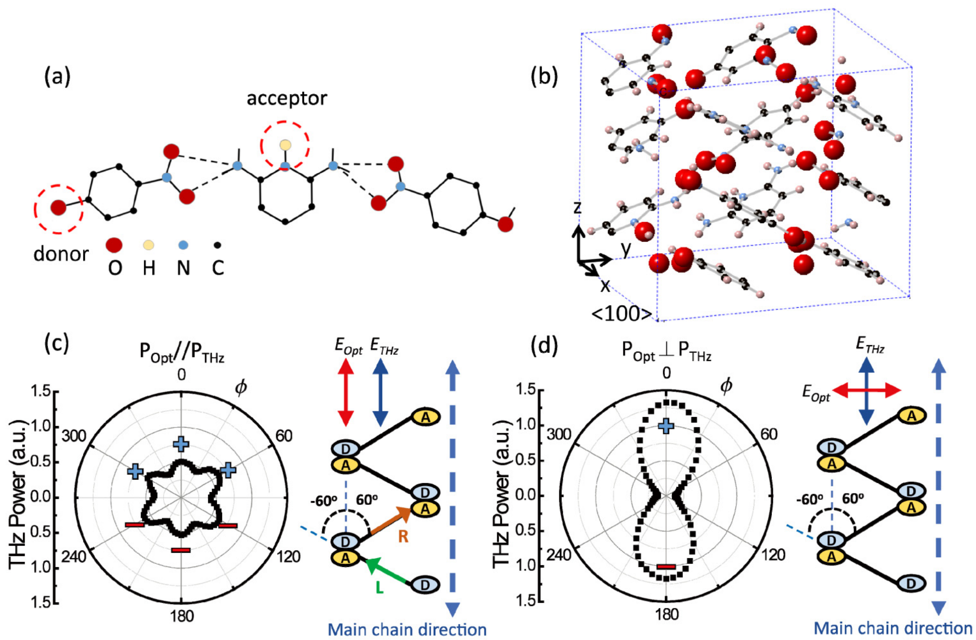

Fig. 2. (a) The molecular structure of DAP$^+$NP$^-$NP. O (red), H (yellow), N (blue), C (black), atoms and H-bonds (black dash line) are shown. (b) The crystal structure of DAP$^+$NP$^-$NP [14]. (c) Left: The azimuthal angle scan (ϕ-scan) of THz power in the configuration of $P_{Opt}//P_{THz}$. The symbols of "+" and "-" represent the polarity state of the corresponding THz waveform. Right: the simplified molecular structure of DAP$^+$NP$^-$NP. The symbols of "A" and "D" represent acceptor and donor atoms, respectively. The dashed line represents the direction of the main chain of DAP$^+$NP$^-$NP. The polarization vectors of L (green) and R (brown) represent the THz radiation generated in ϕ = 300° and 60°, respectively. (d) Left: The azimuthal angle scan (ϕ-scan) of THz power in the configuration of $P_{Opt}{\perp}P_{THz}$. The maximum THz power was generated along the direction of the main chain of DAP$^+$NP$^-$NP.

In order to figure out these interesting ϕ-scan results in DAP$^+$NP$^-$NP crystals, we propose a model based on the strong second-order-nonlinear effect induced by intramolecular charge transfer between electron donor and acceptor of molecules [15]. The simplified molecular structure of a DAP$^+$NP$^-$NP crystal in Figs. 2(a) and 2(b) is shown on the right in Figs. 2(c) and 2(d). The symbols "A" and "D" represent the anionic electron acceptor and the cationic electron donor atoms in Fig. 2(a), respectively, while the dashed line represents the direction of the main chain of a DAP$^+$NP$^-$NP crystal in Fig. 2(b) [12]. After optical excitation, the nonlinear polarization is induced along the molecular chain between the acceptor and the donor. In the $P_{Opt}//P_{THz}$ configuration, the polarization vectors of "L (green)" and "R (brown)" represent the THz wave generated in ϕ = 300° and 60°, respectively. As ϕ = 0°, the induced nonlinear polarizations superimpose and result in a net polarization along the main chain of the DAP$^+$NP$^-$NP molecules. On the other hand, in the $P_{Opt}{\perp}P_{THz}$ configuration, the direction of the maximum THz radiation is also along the main chain of a DAP$^+$NP$^-$NP crystal. All polarities of the measured THz waveform are coincident with the molecular structure of DAP$^+$NP$^-$NP.

#254193 Received 18 Nov 2015; revised 10 Feb 2016; accepted 17 Feb 2016; published 29 Feb 2016

In general, the nonlinear light conversion efficiency in nonlinear optical materials can be brought out significantly through their linear spectra. Therefore, we used a micro-spectrometer, a spectrometer integrated with a commercial optical-microscope, to study the VIS-NIR transmission spectra at three different positions for the used DAP^+NP^-NP crystal as shown in Fig. 3(a). All transmission spectra of these three positions show a cut-off wavelength at ~500 nm and this cut-off wavelength responds to the energy bandgap of the DAP^+NP^-NP crystal. Obviously, the measured transmission spectra in the NIR range show non-negligible differences. At the pumping wavelength, i.e., 800 nm, the measured transmittance at the three positions are 27.0%, 41.5% and 21.8%, which are coincident with the transparencies of these three positions, as shown in the insets of Fig. 3(a). This low percentage of transmission indicates that there are some impurities inside the sample and these undesired impurities reduce the THz generation efficiency.

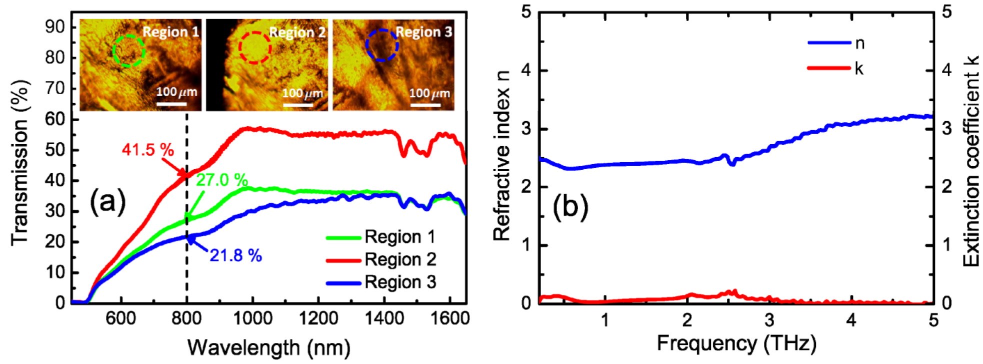

Fig. 3. (a) The VIS-NIR transmission spectra at different positions of the employed DAP^+NP^-NP crystal. The corresponding photos are shown in the insets and the measured areas (spot size) are ~100 μm in diameter. (b) The refractive index and the extinction coefficient of a DAP^+NP^-NP crystal in THz region were obtained by THz time domain spectroscopy. Comparing with Fig. 1(c), DAP^+NP^-NP does not show significant absorption up to 5 THz, which is coincident with the non-distorted few-cycle THz pulse from a DAP^+NP^-NP crystal, as shown in Fig. 1(b).

To estimate the potential of DAP^+NP^-NP crystals for high power THz generation applications, we investigate the effects of thickness and transparency of the samples. First, for the second-order nonlinear optical process, the amplitude of the electric field of THz radiation is directly proportional to both the crystal thickness L and optical pump intensity I_{Opt} inside of the crystal, i.e., $E_{THz} \propto L \times I_{Opt}$ [16]. Second, the undesired impurities inside the samples result in the loss of pumping light and diminish the generated THz intensity (Efficiency is the same since we are claiming that the THz intensity is proportional to the pump intensity). This means the transmitance T of optical pump must be taken into account, i.e., $I_{Opt} \to T \times I_{Opt}$. The spot size (~150 μm) of the pump beam is larger than that (~100 μm) used for micro-transmission spectrum. Therefore, we need to consider that the average transmittance $T_{average}$ and the average value of the transmittance at these three positions is 30.1% ((27.0% + 41.5% + 21.8%)/3 = 30.1%). We estimate that the amplitude of the electric field, $E_{\mathrm{O}\perp\mathrm{T}\text{-}Max}^{\mathrm{DAP^+NP^-NP}}$, of THz radiation from DAP^+NP^-NP in $P_{Opt} \perp P_{THz}$ configuration would be 5.25 (a. u.) ($E_{\mathrm{O}\perp\mathrm{T}\text{-}Max}^{\mathrm{DAP^+NP^-NP}} = E_{\mathrm{O}\perp\mathrm{T}-average}^{\mathrm{DAP^+NP^-NP}} \times \frac{T_{Max}}{T_{average}} \times \frac{L_{1\,\mathrm{mm}}}{L_{0.41\,\mathrm{mm}}} = 1.56 \times \frac{41.5\%}{30.1\%} \times \frac{1\,\mathrm{mm}}{0.41\,\mathrm{mm}} = 5.25$) if a highly transparent (in this study, max transmittance T_{Max} = 41.5%) 1-mm-thick DAP^+NP^-NP is used. This value would be larger than that of 1-mm-thick ZnTe in $P_{Opt}//P_{THz}$ configuration ($E_{\mathrm{O//T}}^{\mathrm{ZnTe}} = 4.5$ (a. u.)). Recently, highly transparent DAP^+NP^-NP crystals with transmittance of

#254193 Received 18 Nov 2015; revised 10 Feb 2016; accepted 17 Feb 2016; published 29 Feb 2016

75% at 800 nm have been reported [13]. This indicates that the amplitude of an electric field twice as large as that from ZnTe could be obtained from a high quality DAP^+NP^-NP crystal. Furthermore, the linear spectrum of DAP^+NP^-NP shows higher transmittance around 1000 nm in the NIR range [13]. Compared with the case using 800-nm optical pulses as the pump, we propose that it is possible to use the optical pumping pulse output from a Yb-doped fiber laser to obtain THz radiation with a high electric field. More detailed information about DAP^+NP^-NP crystals, such as refractive index and absorption coefficient in the NIR range, is necessary for investigating THz applications in the future. In most organic crystals such as DAST, DSTMS and OH1, some resonance absorptions in the THz range result in complex waveform and spectra, which is not preferable for applications. We used THz time-domain spectroscopy to analyze the characteristics of the DAP^+NP^-NP crystal in the THz range. As shown in Fig. 3(b), both the refractive index and extinction coefficient do not show substantial absorbance up to 5 THz in this study. These results are consistent with the observations of non-distorted few-cycle THz pulses from DAP^+NP^-NP crystals and indicate that high quality DAP^+NP^-NP crystals have high potential in THz applications.

4. Summary

In summary, we have examined THz radiation from organic DAP^+NP^-NP crystals by using 800-nm optical pulse excitation. The maximum electric field of THz radiation from DAP^+NP^-NP is comparable to that from 1-mm ZnTe. This indicates that a high quality DAP^+NP^-NP crystal could be a candidate for low cost and high power THz applications.

Acknowledgments

We thank the assistance of C. C. Hong and C. J. Weng for measuring the VIS-NIR transmission spectra. This work was supported by Ministry of Science and Technology (MOST), Taiwan (Contract No. 103-2119-M-009-004-MY3, 103-2628-M-009-002-MY3) and Ministry of Education (MoE) through the Aiming for the Top University (ATU) Program at National Chiao Tung University.